11-13-74

UCRL-51663

OBSERVED PENETRATION OF 14-MeV NEUTRONS IN VARIOUS MATERIALS

C. M. Logan

T. T. Komoto

September 23, 1974

Prepared for U.S. Atomic Energy Commission under contract No. W-7405-Eng-48

LAWRENCE LIVERMORE LABORATORY

University of California/Livermore

MASTER

DISTRIBUTION OF THIS DOCUMENT IS UNLIMITED

NOTICE

"This report was prepared as an account of work sponsored by the United States Government. Neither the United States nor the United States Atomic Energy Commission, nor any of their employees, nor any of their contractors, subcontractors, or their employees, makes any warranty, express or implied, or assumes any legal liability or responsibility for the accuracy, completeness or usefulness of any information, apparatus, product or process disclosed, or represents that its use would not infringe privately-owned rights."

Printed in the United States of America
Available from
National Technical Information Service
U.S. Department of Commerce
5285 Port Royal Road
Springfield, Virginia 22151
Price: Printed Copy $___*; Microfiche $1.45

*Pages	NTIS Selling Price
1-50	$4.00
51-150	$5.45
151-325	$7.60
326-500	$10.60
501-1000	$13.60

TID-4500, UC-34c
Physics—Nuclear

LAWRENCE LIVERMORE LABORATORY
University of California/Livermore, California/94550

UCRL-51663

OBSERVED PENETRATION OF 14-MeV NEUTRONS IN VARIOUS MATERIALS

C. M. Logan
T. T. Komoto

MS. date: September 23, 1974

NOTICE
This report was prepared as an account of work sponsored by the United States Government. Neither the United States nor the United States Atomic Energy Commission, nor any of their employees, nor any of their contractors, subcontractors, or their employees, makes any warranty, express or implied, or assumes any legal liability or responsibility for the accuracy, completeness or usefulness of any information, apparatus, product or process disclosed, or represents that its use would not infringe privately owned rights.

Contents

OBSERVED PENETRATION OF 14-MeV NEUTRONS IN VARIOUS MATERIALS

Abstract

Experimentally observed 14-MeV-neutron removal cross sections are presented for 16 materials. At a scattering energy loss of 4 MeV, the effective macroscopic cross section per unit mass (cm^2/g) for a nucleus of mass A is given by $0.25A^{-1.78} + 0.10A^{-0.47}$. Such information provides a simple method for estimating neutron transport in systems driven by thermonuclear neutrons.

Introduction

The data presented here provide a simple and versatile method for estimating the neutron transport in systems driven by 14-MeV neutrons. The transport of 14-MeV neutrons through materials is of great importance in many fields; for example, the design of nuclear weapons, the prediction of the effects of nuclear weapons, the design of neutron radiotherapy systems, the design of fusion reactors, and the assurance of personnel safety near 14-MeV-neutron generators.

The attention given to biological and energy-producing applications has increased recently, and it will probably continue to increase in the future. Sophisticated and costly analytical techniques such as Monte Carlo transport codes are used in these applications; however, in some cases a less elaborate approach would suffice, and in many others the design process would be facilitated if a simple scheme for providing approximate 14-MeV-neutron transport data were available. This report presents such data for a wide variety of commonly used engineering materials.

The Experiments

The Livermore pulsed-sphere experiments were conceived to provide integral data against which transport codes and data sets could be tested. The nature of this program is outlined elsewhere[1] and will not be fully described here. In these experiments, nearly spherical assemblies of various materials are pulsed at the center with a short burst of 14-MeV neutrons. (The neutrons are generated by directing a deuteron beam on a small tritium target near the center of the sphere.) A neutron detector is positioned several meters away, and a "time

spectrum" is recorded of the number of detected neutrons versus the neutron time of flight. The sphere radius is small compared with the neutron flight path, and the detection efficiency of the detector for neutrons of various energies is well known. The neutron velocities are determined from the measured time spectrum, and the neutron-energy spectrum may then be directly calculated from the velocities. Cramer et al.[2] have shown that the energy spectrum above 2 MeV calculated in this manner has negligible error for the LLL pulsed-sphere geometry.

At thicknesses up to a few mean free paths for 14-MeV neutrons, this "neutron-leakage" spectrum is observed to be separable into two groups: 1) a "transmitted peak" of neutrons whose energy is still near the source energy, and 2) neutrons which have been scattered to significantly lower energies. (After traversing through some material, only a portion of the neutrons in the transmitted peak are in fact virgin neutrons; some have undergone one or more scattering events but have given up only a small fraction of their kinetic energy.)

For each pulsed-sphere experiment, a "blank" run was made to determine the effects of air and of any necessary containers for the material being studied. With such effects accounted for, the experiments represent, to a very good approximation, the neutron transmission properties of the materials under investigation.

Results

FORMAT

We have determined three dimensionless parameters for each pulsed-sphere experiment. The three parameters, N_{pk}, N_t, and E_t, are defined as follows:

$$N_{pk} = N_1/N_0,$$
$$N_t = N_2/N_0,$$
$$E_t = E_1/E_0,$$

where

N_1 = the number of detected neutrons with an energy greater than $(E_s - 4.0)$,

E_s = the energy of the source neutrons in MeV,

N_0 = the number of neutrons detected in the absence of the sphere,

N_2 = the number of neutrons detected with an energy greater than 2.0 MeV,

E_1 = the energy emitted by the sphere as kinetic energy of neutrons with an energy greater than 2.0 MeV,

E_0 = the energy of the source neutrons emitted in the absence of the sphere.

These parameters for 16 materials are presented in Figs. 1-16 as plots of leakage fraction versus material thickness. The ordinates (leakage fraction) are logarithmic, with tick marks on the integers; the abscissas (material thickness) are linear, calibrated in units of centimeters and grams per square centimeter. The measured-data points are connected by straight lines.

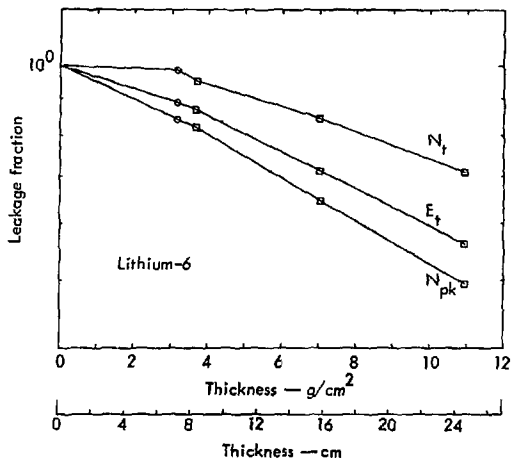

Fig. 1. Transmission parameters for lithium-6.

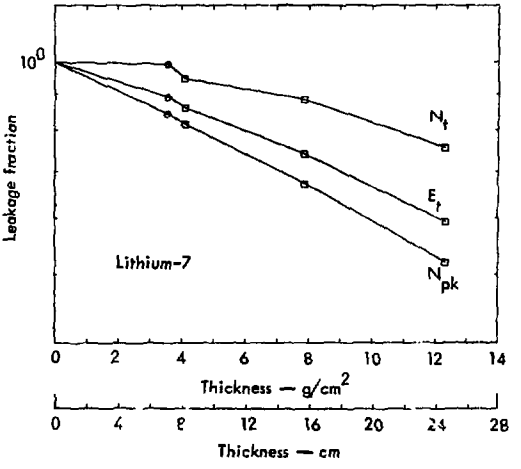

Fig. 2. Transmission parameters for lithium-7.

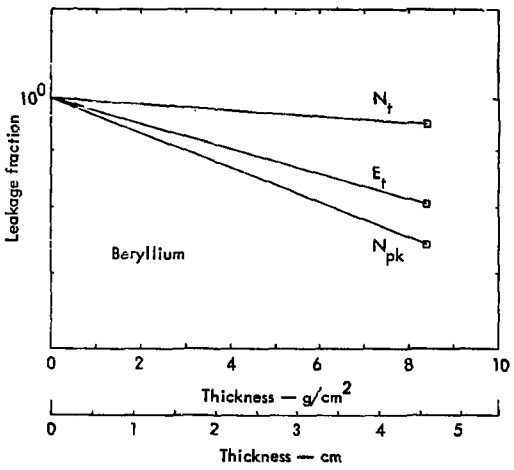

Fig. 3. Transmission parameters for beryllium.

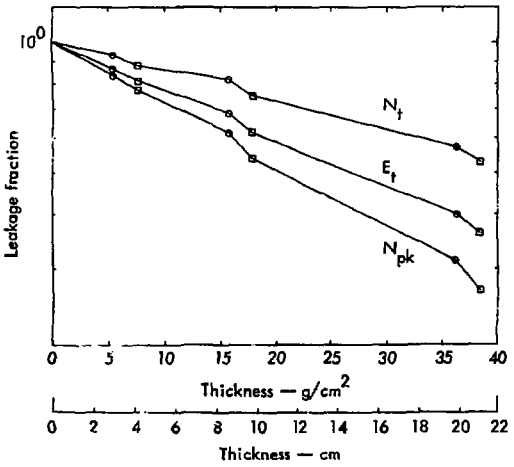

Fig. 4. Transmission parameters for carbon.

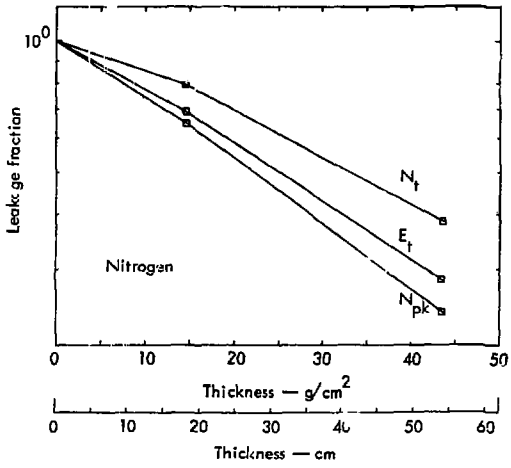

Fig. 5. Transmission parameters for nitrogen.

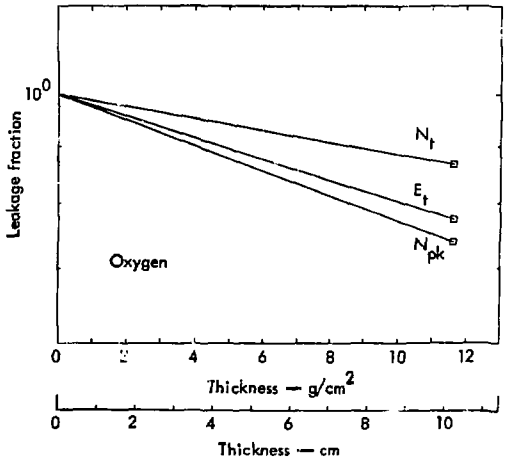

Fig. 6. Transmission parameters for oxygen.

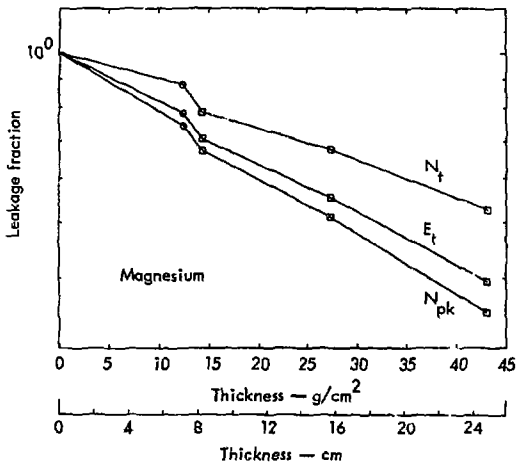

Fig. 7. Transmission parameters for magnesium.

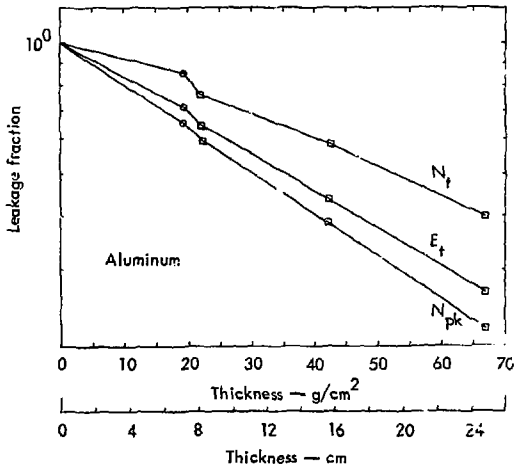

Fig. 8. Transmission parameters for aluminum.

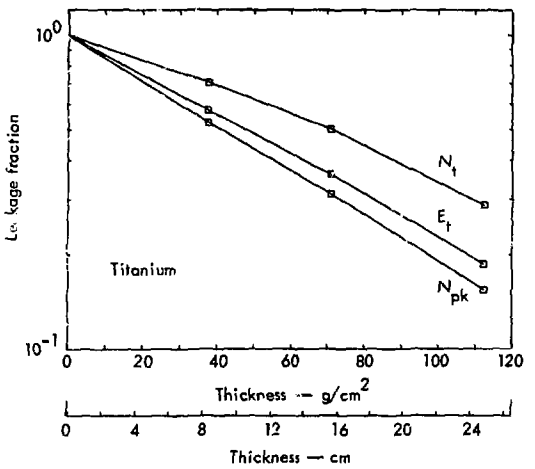

Fig. 9. Transmission parameters for titanium.

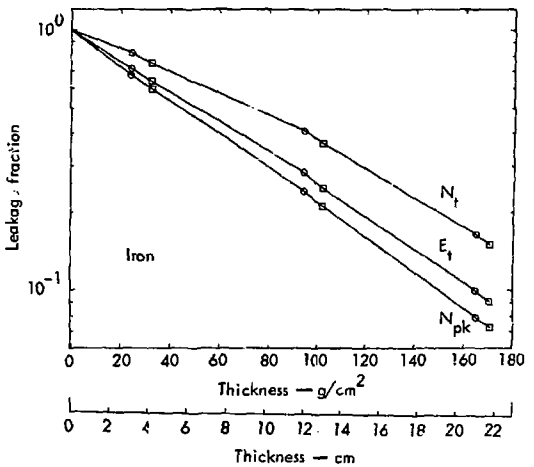

Fig. 10. Transmission parameters for iron.

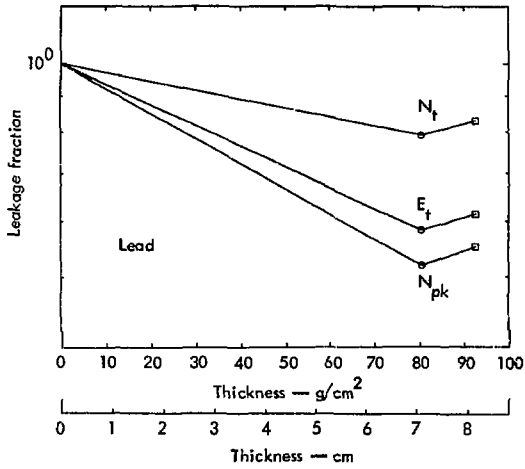

Fig. 11. Transmission parameters for lead.

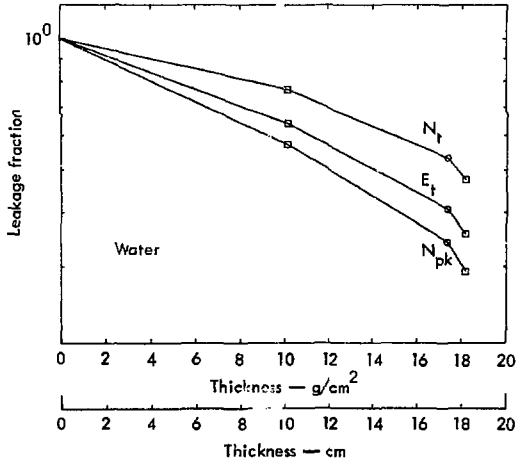

Fig. 12. Transmission parameters for water.

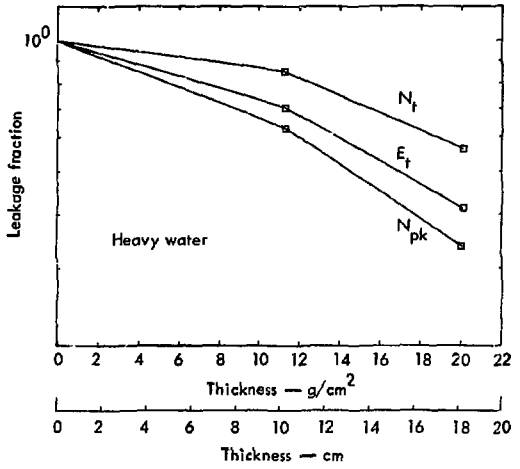

Fig. 13. Transmission parameters for heavy water.

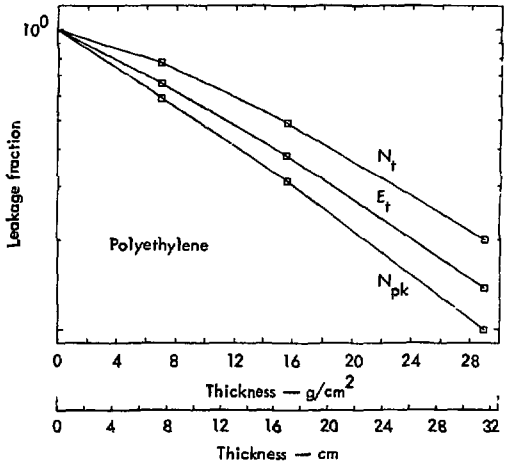

Fig. 14. Transmission parameters for polyethylene.

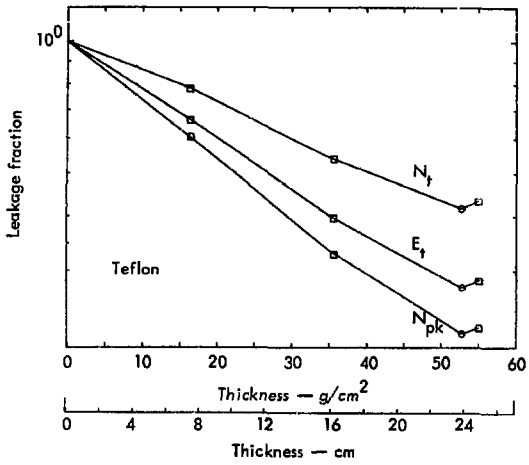

Fig. 15. Transmission parameters for Teflon.

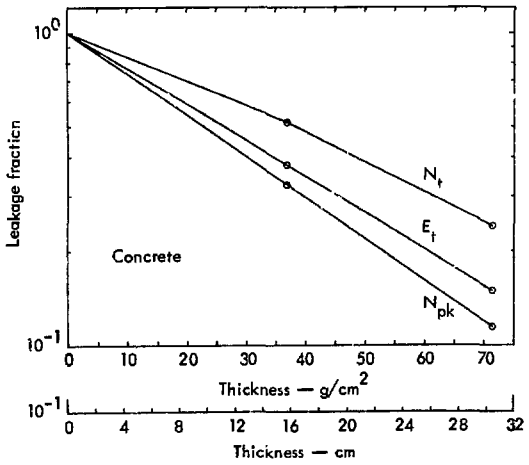

Fig. 16. Transmission parameters for concrete.

Data were taken at angles of 30° and 120° from the direction of the incident deuteron beam. For this neutron source, the most probable source energies at these angles are 14.97 and 13.65 MeV, respectively.[1] Data from the 120° position are denoted by circles, and data from the 30° position are denoted by squares.

REMARKS ON THE DATA

Beryllium (Fig. 3)—The data for beryllium were taken at only one angle and thickness.

Carbon (Fig. 4)—The data for carbon exhibit systematically higher transmission in the backward direction (120°). This effect is real and is consistent with the physics of the scattering processes. The detector at the 120° position sees unscattered neutrons with energies of about 13.6 MeV, but the energy of forward-angle (30°) neutrons from this source is almost 15 MeV. Elastically scattered neutrons therefore arrive at the 120° detector with energies greater than 10.8 MeV and are included in N_{pk}. In the spectrum taken at 30°, however, this effect causes elastically scattered neutrons to fall below (E_s - 4.0), and the resulting integrals are therefore slightly lower. Data on neutrons from a monoenergetic 14.1-MeV source would fall between these two measurements.

Nitrogen (Fig. 5)—Nitrogen was measured at only one angle for two spheres.

Oxygen (Fig. 6)—Only one oxygen measurement was made.

Iron (Fig. 10)—The iron data were taken at both angles for a set of three spheres ranging up to 0.2 m in radius. These data have been extensively utilized and carefully checked.

Lead (Fig. 11)—Lead was measured at two angles for one sphere. The two measurements are inconsistent. The most probable explanation is a void in the neutron path in the forward direction. The forward-angle measurement was not used in determining the effective removal cross sections.

Application of the Data

Values for the removal cross sections based on N_{pk}, E_t, and N_t are given in Table 1. These values minimize the squares of the deviations of the cross sections. The cross section for removal of neutrons from the high-energy peak is plotted versus atomic weight in Fig. 17. The value for hydrogen is determined from water and polyethylene, the value for deuterium from heavy water, and the value for fluorine from Teflon. The value for concrete is consistent with the values for its constituents.

These cross sections are well represented by

$$\Sigma/\rho = 0.25A^{-1.78} + 0.10A^{-0.47}, \quad (1)$$

where Σ/ρ is the removal cross section per unit mass (cm^2/g) and A is the mass of the target nucleus in atomic mass units.

Table 1. Experimentally observed removal cross sections.

Material	Removal cross section per unit mass, Σ/ρ (cm^2/g)					
	For removal from high-energy peak		For neutron kinetic energy above 2 MeV		For downscattering below 2 MeV	
	Σ/ρ	Av deviation	Σ/ρ	Av deviation	Σ/ρ	Av deviation
Lithium-6	0.0611	0.0045	0.0476	0.0060	0.0233	0.0094
Lithium-7	0.0511	0.0019	0.0390	0.0034	0.0167	0.0063
Beryllium	0.0354	–	0.0258	–	0.0060	–
Carbon	0.0331	0.0012	0.0259	0.0009	0.0154	0.0014
Nitrogen	0.0321	0.0017	0.0281	0.0017	0.0204	0.0031
Oxygen	0.0362	–	0.0221	–	0.0123	–
Magnesium	0.0249	0.0012	0.0218	0.0013	0.0144	0.0018
Aluminum	0.0227	0.0003	0.0195	0.0007	0.0126	0.0015
Titanium	0.0166	0.0003	0.0147	0.0002	0.0104	0.0008
Iron	0.0153	0.0003	0.0099	0.0047	0.0103	0.0012
Lead	0.0081	–	0.0067	–	0.0029	–
Water	0.0627	0.0044	0.0521	0.0042	0.0360	0.0051
Heavy water	0.0494	0.0067	0.0395	0.0065	0.0234	0.0072
Polyethylene	0.0778	0.0022	0.0656	0.0039	0.0504	0.0076
Teflon	0.0292	0.0014	0.0244	0.0011	0.0162	0.0009
Concrete	0.0304	0.0030	0.0265	0.0027	0.0193	0.0019

The data presented here can be used with high confidence for spherical assemblies over the range of thicknesses measured; the pulsed-sphere experiments are reproducible within a few percent. If applied reasonably and with appropriate caution, they can also be used for other geometries.

The effect of cylindrical or slab geometry can be estimated analytically. We see from the data that the attenuation of N_{pk} is approximately exponential. Assuming exponential attenuation of N_{pk}, the fraction F of neutrons leaking from a cylinder with a line source at the center is given by

$$F_{cyl} = \int_0^{\pi/2} e^{-x/\cos\theta} \cos\theta \, d\theta, \quad (2)$$

where x is the radius of the cylinder in mean free paths, and θ is measured from the cylinder axis. The fraction leaking from a slab with a line source at the center is

$$F_{slab} = \int_0^{\pi/2} e^{-x/\cos\theta} \cos\theta \sin\theta \, d\theta, \quad (3)$$

where x is the half-thickness of the slab in mean free paths, and θ is measured from the slab center line. In Fig. 18, the ratios of the leakages from these two geometries to the leakage from a simple sphere with exponential attenuation are plotted as functions of thickness. Such geometric corrections could easily be evaluated for other specific problems.

As an example to illustrate the power of this kind of data, we have chosen the

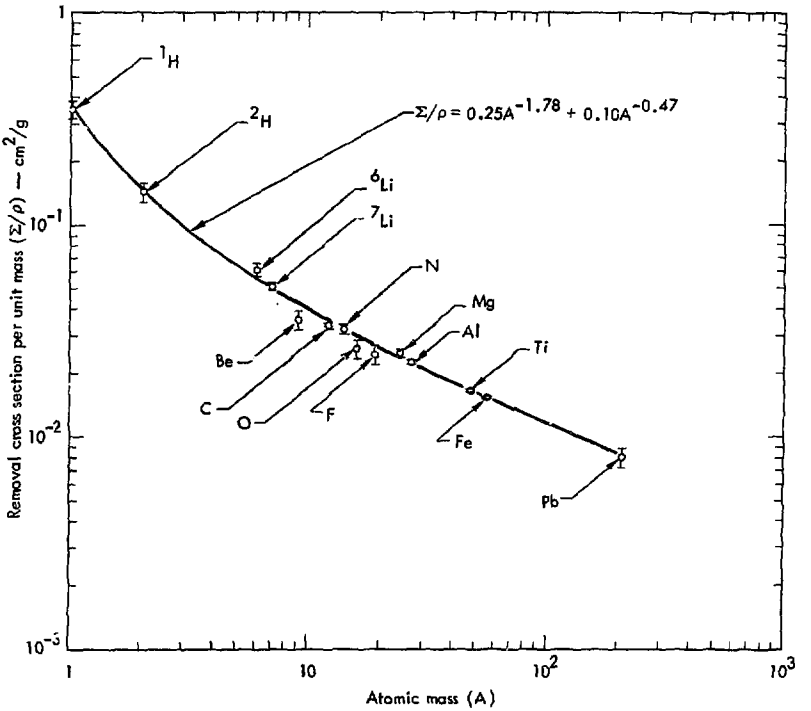

Fig. 17. The removal cross section per unit mass (Σ/ρ) vs the atomic mass (A) of the scattering nucleus. The cross section is for a 4-MeV energy loss from a thermonuclear neutron.

"standard blanket" for controlled thermonuclear reactors. This geometry was chosen in 1971 for use as a "benchmark" in comparing different transport codes. A summary and analysis of the results has been given by Steiner[3] for the United States contribution. Steiner also gives the detailed geometry and materials of the standard blanket.

The source-and-blanket system is an infinite cylinder, with a source zone of 1.5 m radius and the blanket beginning at 2.0 m radius and extending to 3.0 m. The blanket contains lithium, niobium, and carbon. Using the thicknesses of the materials as taken from Ref. 3 and the cross-section data given in Table 1, we can find the N_{pk} values for each material. (The cross section for niobium is calculated from Eq. 1.) These thicknesses and N_{pk} values are listed in Table 2.

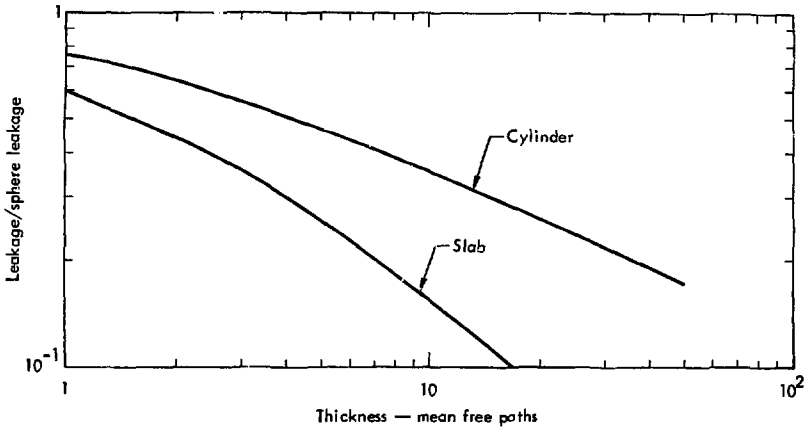

Fig. 18. Ratio of the calculated leakage from a line source centered in a slab and in a cylinder to the leakage from a sphere, assuming exponential attenuation.

The product of these N_{pk} values is 0.020, indicating 3.9 mean free paths. Figure 18 indicates that the cylinder-to-sphere leakage ratio at 3.9 mean free paths is about 0.5. Thus, these data predict that about 0.01 high-energy neutron should leak from the standard blanket for each 14-MeV source neutron. This result represents an upper limit, since it does not account for the cylindrical source geometry or for the softening of the hard component as it is propagated through the thick blanket.

For comparison, we can cite two more-detailed calculations of the same geometry. Investigators at the University of Wisconsin[4] have calculated this geometry with a discrete-ordinates code and the ENDF/BII data set; they calculate 0.0034 leakage neutron with energy greater than 8 MeV. At LLL, we have calculated this geometry with the TART Monte Carlo code[5] and the Livermore Evaluated Data set[6]; this calculation predicts 0.0025 neutron leaking with energy above 8 MeV.

Table 2. Transmission results.

Material	Thickness (g/cm^2)	N_{pk}
Carbon	48.09	0.20
Niobium	44.12	0.59
Lithium-6	2.19	0.87
Lithium-7	32.39	0.19

As a more direct comparison of the pulsed-sphere data with TART, we have calculated a 0.2-m-radius iron sphere with an isotropic 14.1-MeV point source at the center. TART calculates 0.09 leakage neutron with an energy greater than 8 MeV, which agrees with the pulsed-sphere data. If we wished to calculate the leakage from a 0.4-m-thick slab with

a centered source, we see that a transmission of 0.09 corresponds to 2.4 mean free paths, and that Fig. 18 indicates the slab should have 0.4 of the leakage from a sphere. The pulsed-sphere data then predict a leakage of 0.036. A TART calculation for an infinite slab predicts 0.021.

Caution is required when applying these data to the design of biological shields and collimators. These attenuation data do not represent dose attenuations. It is possible to get partial dose information from these data by applying appropriate KERMA factors to the separate high-energy and low-energy neutron components, but the contributions from neutrons below 2 MeV and from gamma radiation will not be included. In some systems, this may represent a significant omission.

This technique cannot be applied to extremely thick systems. With increasing penetration, the neutron spectrum softens, and the leakage is no longer exponential. At thicknesses greater than 5 mean free paths, the pulsed-sphere data can only serve as a rough design aid.

Acknowledgments

This work was made possible by the support and encouragement of Dick Stone, Gene Goldberg, and John Anderson.

References

1. C. Wong, J. D. Anderson, P. Brown, L. F. Hansen, J. L. Kammerdiener, C. M. Logan, and B. A. Pohl, Livermore Pulsed Sphere Program, Program Summary through July 1971, Lawrence Livermore Laboratory, Rept. UCRL-51144 Rev. 2 (1971).
2. S. N. Cramer, R. W. Roussin, and E. M. Oblow, Monte Carlo Calculations and Sensitivity Studies of the Time-Dependent Neutron Spectra Measured in the LLL Pulsed Sphere Program, Oak Ridge National Laboratory, Rept. ORNL-TM-4072 (1973).
3. D. Steiner, Analysis of a Bench-Mark Calculation of Tritium Breeding in a Fusion Reactor Blanket: The United States Contribution, Oak Ridge National Laboratory, Rept. ORNL-TM-4177 (1973).
4. University of Wisconsin Fusion Feasibility Study Group, UWMAK-I, a Wisconsin Toroidal Fusion Reactor Design, University of Wisconsin, Rept. UWFDM-68 (1973).
5. E. F. Plechaty and J. R. Kimlinger, Lawrence Livermore Laboratory, Internal Rept. UCIR-522 (1971). Readers outside the Laboratory who desire further information on LLL internal documents should address their inquiries to the Technical Information Department, Lawrence Livermore Laboratory, Livermore, California 94550.
6. R. Howerton, R. J. Doyas, T. C. Michaels, and S. T. Perkins, Evaluated Nuclear Cross Section Library, Lawrence Livermore Laboratory, Rept. UCRL-50400, Vol. 4 (1971).

GRS/bl